Fusion Engineering and Design 180 (2022) 113193

Contents lists available at ScienceDirect

Fusion Engineering and Design

journal homepage: www.elsevier.com/locate/fusengdes

HIDRA-MAT liquid metal droplet injector for liquid metal applications in HIDRA

A. Shone [a,*], Z. Koyn [b], B. Kamiyama [a], E. Perez [a], L. Barrus [a], N. Bartlett [a], J.P. Allain [c], D. Andruczyk [a]

[a] University of Illinois Urbana-Champaign, Urbana IL, United States
[b] Energy Driven Technologies LLC, Champaign IL, United States
[c] Pennsylvania State University, State College PA, United States

A B S T R A C T

A liquid metal droplet injector was explicitly designed for the Hybrid Illinois Device for Research and Applications Material Analysis Test-stand (HIDRA-MAT) at the University of Illinois Urbana-Champaign to prepare liquid metal plasma-facing components (PFCs) for plasma exposure. The design goals were to create a compact, reliable, and robust design that could apply liquid metal droplets *in-vacuo* to a variety of samples. The injector was designed for liquid metal use, and results discussed pertain to lithium. The injector can produce lithium droplets of consistent size by utilizing programmable piston movement. Droplet formation data is presented for four different piston step sizes (0.125 mm, 0.25 mm, 0.5 mm, and 1 mm) at three different nozzle temperatures (185 °C, 230 °C, and 270 °C). Droplets are formed on the injector nozzle tip and a linear shift mechanism vertically translates the droplet to the substrate for application. This design prevents the droplet from inadvertently detaching off the nozzle and falling to the sample. Application of the liquid metal droplet ensures placement consistency on the substrate and helps avoid damage to components in HIDRA-MAT that should not interact with liquid metals. A description of the liquid lithium droplet creation and application results is given and provides additional insight into the cooling and oxidation of lithium droplets under vacuum conditions. A second nozzle was fabricated and demonstrated repeatability in droplet diameter creation having a variance of ±0.14 mm for droplets created from the same number of piston steps. The end-use for the injector on HIDRA-MAT is to apply liquid metals to PFCs and expose them to HIDRA's plasma with subsequent intershot *in-vacuo* surface analysis in HIDRA-MAT for plasma-material interaction studies.

1. Introduction

Plasma-facing components (PFCs) in fusion devices will have to withstand a harsh environment over an extended period of time for commercial fusion energy to become a reality. Traditionally relied upon solid PFCs face significant challenges in the high-temperature, high-radiation fusion plasma environment. Extreme particle fluxes induce changes to solid PFCs, such as embrittlement, structural changes, and surface morphology (e.g., fuzz and blister growth [1]) that enhance mechanical failure mechanisms and impurity sputtering or macroscopic erosion into the plasma that can disrupt or even halt a sustained reaction. In addition, solid PFCs retain tritium fuel via plasma-material interactions (PMI), further disrupting sustainability of the fusion reaction and causing maintenance challenges with the device after extensive operation.

Due to these properties of solid PFCs, liquid metals are being investigated as a potential alternative. In particular, liquid lithium has gained popularity due to some of its advantageous properties. Lithium is a low-Z material, has been shown to reduce the recycling rate of plasma impurities, and increases overall plasma performance when introduced in a device [2,3]. Furthermore, liquid metal walls are self-healing and have the potential ability to self-pump through experimentally proven concepts like thermoelectric magnetohydrodynamic driven flow [4]. Ultimately, liquid metals could be incorporated into a flowing loop system that can be used, in the case of lithium, for extraction of DT fuel and other impurities. These properties and potential applications motivate the focus of fusion PMI research toward liquid metal PFCs.

There are various ways to introduce lithium into a fusion system. Some setups use lithium evaporation for conditioning of the walls to coat the inside of the machine [5], while others inject lithium granules to target the plasma itself [6]. Specific injection systems can also introduce a powder that interacts with a plasma column, which turns it into an aerosol inside the scrape-off layer [7]. These systems help increase plasma performance and provide further evidence supporting the use of lithium in fusion devices.

PMI research is critical to developing future plasma-burning nuclear

* Corresponding author.
E-mail address: shone2@illinois.edu (A. Shone).

https://doi.org/10.1016/j.fusengdes.2022.113193
Received 23 September 2021; Received in revised form 28 April 2022; Accepted 29 May 2022
Available online 2 June 2022
0920-3796/Published by Elsevier B.V.

fusion reactors, including a more extensive study of plasma-liquid lithium interactions. Wetting experiments involving liquid lithium applied to underlying substrates have been conducted using droplet injectors to investigate liquid lithium properties [8,9]. Wetting experiments produce fundamental data on liquid metal-substrate interactions such as wetting temperatures, material choice, geometric configurations, etc., for the design of liquid metal PFCs. Useful data on lithium behavior can be extracted from these experimental results, but there is still a lack of supporting *in-vacuo* diagnostics to develop a more complete understanding of the liquid metal-substrate interactions at play. Furthermore, no other system currently exists with the capability of controllably introducing liquid metal to sample surfaces *in-vacuo* prior to plasma exposure. In this work, a new liquid metal droplet injection system is introduced along with its integration into the Hybrid Illinois Device for Research and Applications Material Analysis Test-stand (HIDRA-MAT) [10] to provide a deeper understanding of liquid metal-substrate and plasma-liquid metal-substrate interfaces.

2. Liquid metal droplet injector design

2.1. LMDI design

The liquid metal droplet injector (LMDI) design drew inspiration from UIUC and UCSD injectors that performed similar tasks [8,9]. The injectors discussed herein refer to 'single-droplet' injectors. This type of injector aims to produce single droplets at a time for sample preparation or wetting experiments, as opposed to multiple droplets being produced at a specific frequency for injection into a plasma core. The injector UIUC used in the lithium-tungsten contact angle experiment employed argon back-pressure to produce the lithium droplets, cartridge heaters for heating, and provided no further information on injector design components. The UCSD injector used a manual linear bellows drive with a piston-O-ring combination for injection, MgO insulated heater coax for heating, and an exit nipple or tubular extension tip for the nozzle.

Though similar, HIDRA-MAT's LMDI was specifically developed for use on the HIDRA-MAT chamber and required compatibility with HIDRA-MAT's sample preparation components and diagnostics. In HIDRA-MAT, samples are held in place on a UHV heater that is at a fixed height during the droplet application. The setup demands droplet placement accuracy to avoid applying liquid metal onto heater electronics and possibly destroying them from corrosive interaction so thus, a single-droplet injector is required. Samples can be up to 25 mm in diameter and 6 mm in height. Varying sample heights necessitates the LMDI to be capable of applying droplets consistently irrespective of sample geometry. Compactness of the injector design allows for ease in LMDI handling such that loading and installation can be done by one person. Modularity in design allows for cost-efficient repair or replacement when required because components can be separated from one another.

The design shown in Fig. 1 highlights how the injector components come together in the final assembly. Assembly involves attaching the linear bellows drive (LBD) to the atmospheric side of the custom mounting flange. The reservoir piston screws into the LBD and the liquid metal reservoir slides over the piston and connects to the vacuum side of the custom mounting flange. The heating coil slides over the reservoir tightly for good thermal contact, and the heating coil leads connect to the thermocouple/power feedthrough. Solid metal is loaded through the end of the liquid metal reservoir. A glove-box argon environment with $<$ 8% oxygen content is used when loading solid lithium to mitigate oxidation. The reservoir assembly has a loading volume of ~6.6 cm^3, which equates to ~3.5 g of lithium. Depending on experimental conditions (temperature, step size, etc.), the number of drops that can be created from a full load varies and will be discussed later on. After loading the solid metal, the reservoir nozzle is screwed onto the end of the reservoir, and the injector is installed onto the actuated linear shift mechanism (LSM), which remains on the HIDRA-MAT chamber. Once the custom flange is tightened onto the LSM, HIDRA-MAT is pumped down. Supporting electronics and power supplies for the actuation and data collection are connected, and the injector is ready for use.

The HIDRA-MAT vacuum chamber, shown in Fig. 2, is pumped down to pressures of 4×10^{-4} Pa [3×10^{-6} Torr] or lower for droplet creation. In the case of lithium, the heater is brought to the target temperature as measured by the thermocouple inside of the coil heater. The minimum temperature for droplet creation ($T_{melt,\ Li} = 180.5\ ^{\circ}C$) can be reached in ~1 hour depending on heater ramp rate. Slower ramp rates that take between 3–6 h to reach target temperature are set to ensure even heating from nozzle tip to the reservoir and to avoid damage to the heater. The actuated LBD controls the movement of the reservoir piston that pushes the liquid metal out of the reservoir nozzle to create a droplet. The distance from the nozzle to the substrate surface can be adjusted by moving the LSM in the z-direction. The transfer arm controls the rotation and positioning of the sample in HIDRA-MAT.

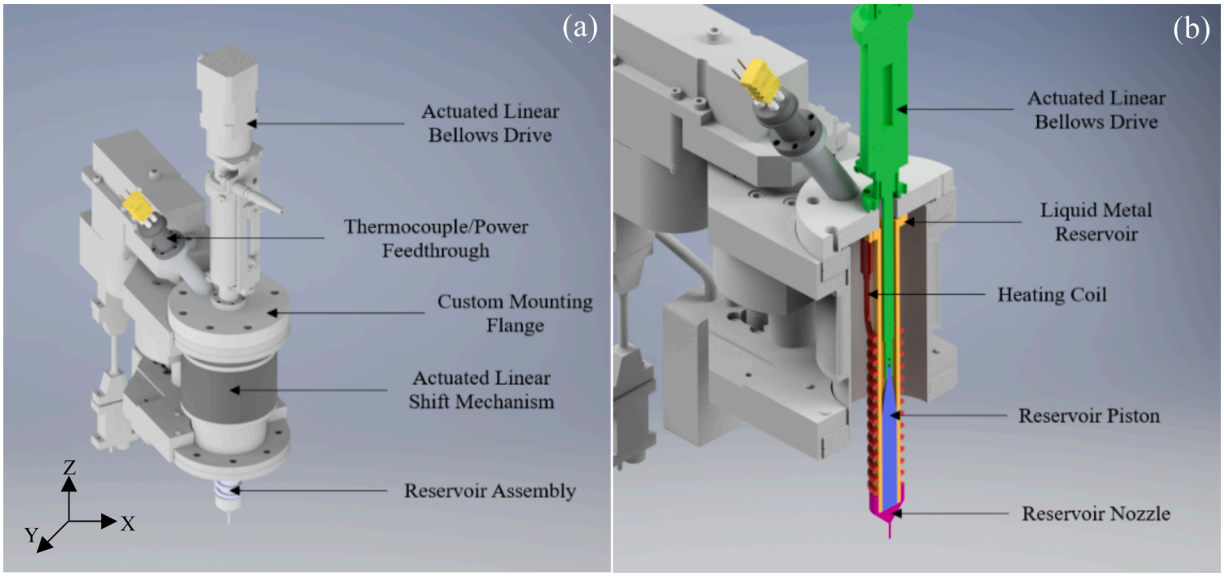

Fig. 1. CAD drawing of the original HIDRA-MAT LMDI design showing (a) the main components and (b) the cross-section of the reservoir assembly when performing injection.

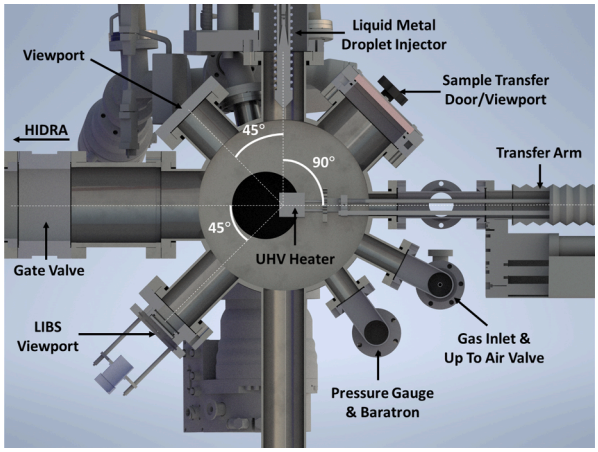

Fig. 2. CAD of the HIDRA-MAT main chamber setup. The UHV heater is rotated 90° so the LMDI can apply the liquid metal to the substrate surface. The heater is then rotated 90° back to horizontal for plasma exposures in HIDRA.

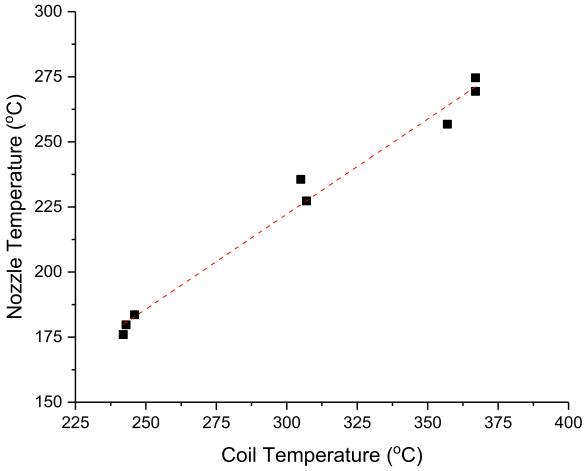

Fig. 3. A relationship between nozzle tip temperature and heating coil temperature is shown above. Measurements were taken between pressures of 2–3 $\times$ 10^{-6} Torr.

2.2. Component details

The LMDI builds upon existing injector designs [8,9] and introduces expanded utility through its unique component designs. In particular, the LMDI's actuated movement, custom heating coil, and reservoir assembly come together to create a compact, reliable, and robust design. Each component is discussed in depth and provides justification for each design choice as well as being compared and contrasted with other single-droplet injectors.

2.2.1. Actuated movement

Versatility and safety are inherent to the LMDI design and originate from the injector's actuation. Component movement can be controlled from a safe distance by running set programs from a control computer. The LSM is an LSM64–50-SADC with 50 mm of travel, enabling droplet application to samples of various thicknesses. It is also possible to apply a droplet to the sample without it detaching from the nozzle and falling to the sample. Physically dropping the liquid metal onto the substrate could cause unwanted droplet breakup onto heater components. The LSM stays installed on the vacuum chamber by a DN63CF (4.5″) connection, and all other components are attached via the DN63CF mounting flange after the metal has been loaded in the reservoir. The other actuated component is an LBD16–50-IS with 50 mm of travel and a DN16CF (1.33″) connection. At the full stroke length, the piston's position is at the end of the reservoir, reducing metal waste. This programmable actuation in the LBD gives the LMDI more versatility in droplet formation and application compared to the other single-droplet injectors because step size can be chosen. Repeatable piston movement and stroke lengths, the motorized LBD has a resolution of one micron, allow for droplet size to be controlled. Movement of the LSM and LBD have limited vibrational effect on the assembly and what vibration is present had no observable influence on droplet formation. The other single-droplet injectors mentioned either used argon back-pressure or a manually controlled piston.

2.2.2. Heating coil system

Heating is achieved by a custom TEMPCO Mightyband Coil Heater with a built-in type K thermocouple surrounded by MgO insulation. The heater can reach temperatures above 1000 °C, though a maximum of 375 °C is required for this application. Heating tests have been carried out to relate nozzle temperature to the temperature of the heating coil and the data is presented in Fig. 3. Copper shim is wrapped around the nozzle to promote heat transfer to the nozzle tip. There is no interaction between lithium and copper in this design, preventing copper alloying or corrosion. A thermocouple was placed on the nozzle tip during installation and was removed *in-vacuo* the moment before droplet testing. A linear relationship can be seen between coil and nozzle temperature. Nozzle temperature has a slight dependence on pressure. Lower pressure allows for better heating, so each data point was recorded at a similar pressure value (2–3 $\times$ 10^{-6} Torr). The compact design of the injector and its coiled heater allows for efficient and uniform heating of the liquid due to its smaller size.

The power and thermocouple leads are covered by a 304SS sheath, except for the connection points to the feedthrough. Connections are covered in Kapton tape during installation for electrical isolation. The coil fits tightly around the liquid metal reservoir but has enough flexibility to be removed. The nozzle prevents the coil from sliding down the reservoir and aids heat transfer to the nozzle as it is in direct contact with the heating coil. The heater's power and thermocouple leads connect to the power supply and thermocouple reader through a feedthrough. The thermocouple is located at the end of the coil and rests on the top of the nozzle. The placement of the thermocouple gives a general idea of the liquid metal temperature in the reservoir but is not the metal's true temperature. It has been observed that the nozzle tip takes longer to heat up than the reservoir due to the poor thermal conductivity of stainless steel. The molten metal in the reservoir and nozzle also helps with heat transfer to the nozzle tip.

2.2.3. Reservoir assembly and injection of droplets

The reservoir assembly is comprised of the liquid metal reservoir, reservoir piston, reservoir nozzle, and heating coil. These components attach to the custom mounting flange and the actuated LBD for liquid metal droplet injection. Keeping lithium use in mind, the design accommodated all reservoir assembly components to be made out of 304SS for stronger corrosion resistance. Each component can be separated from one another for ease of cleaning. If a component needs to be repaired or replaced, the whole injector does not have to be replaced, saving cost over time.

The liquid metal reservoir (9″ length, ~0.5″ ID) is a bored-out ¾” 304SS rod threaded at one end, and a DN16CF connection welded onto the other. The threads on the outside of the reservoir help slow lithium from creeping up the nozzle walls and spilling into the vacuum chamber. If the threading were on the inside of the reservoir, gravity would aid lithium creep, and lithium could cover the outside of the nozzle. The reservoir dimensions were purposely chosen to keep the assembly compact and limit the amount of material used in case the reservoir had to be repaired, replaced, or duplicated. The piston has a cylindrical design that tapers at the top to an 8 mm long M4 thread so it can be attached to the LBD. Piston length was designed ensuring the maximum

amount of lithium could be loaded along with the smallest amount of waste. A total length of 113 mm from piston base to the top of the piston leaves 50 mm between piston base and nozzle base when the piston is at its home position. The piston diameter is machined to a 0.51″ diameter then undergoes further machining until the point where it starts to have movement up and down the reservoir. If there is enough space between the reservoir wall and the piston, lithium will make its way up the piston when force is applied rather than out of the nozzle tip.

The nozzle's design evolved from previous designs used on other injectors at UIUC [8]. There have been two nozzle designs employed on this specific injector. Fig. 4a shows the first nozzle design. This design was made from a 1″ 304SS rod and had a total length of 1.5″. The piston forced lithium through a 1″ long, 1/32″ diameter channel. The nozzle tip has a 1/16″ outer diameter. This tip diameter was chosen from previous UIUC nozzle tip diameters. The nozzle tip diameter selected was one that produced large enough droplets for HIDRA-MAT sample preparation along with being durable for use in multiple tests. The nozzle was also machined for a 7/8″ wrench to be used for tightening onto the reservoir. This nozzle design worked well but was not without flaws. The significant issues that arose were lithium clogging in the long channel and thread damage. Cleaning immediately after venting to atmosphere did not prevent lithium oxides from forming and clogging the channel. Unclogging proved to be tedious and time-consuming. Additionally, the threading extended all the way to the nozzle base, and over time, lithium damaged the threads. The threads were repaired once before the second nozzle was fabricated. Fig. 4b shows the second nozzle design which aimed to eliminate these issues. It must be noted that the reservoir was shortened to a length of 8.5″ in order to fix damaged threads. The second nozzle was designed to keep the same overall length and loading capacity as the previous assembly. To avoid clogging, the single channel was shortened and split into two channels. The longer channel diameter was increased to 1/16″ but the nozzle orifice was kept the same at a 1/32″ diameter. Widening of the channel prevented clogging and made cleaning much easier. Secondly, the threading length was reduced so there was reduced threat that lithium creep would damage the threads. Little to no creep has been seen, and there has been no damage to the threads after multiple uses with the new design. The observations on lack of creep with the second nozzle design may be attributed to the orifice being below the point where the reservoir-nozzle interface is. In the first nozzle design, the pressure the piston exerted on the liquid lithium could have driven the lithium in between the reservoir-nozzle interface and towards the threads. A larger exit channel in the second nozzle paired with the raised reservoir-nozzle interface may be more favorable for lithium injection. This suggests lithium would preferably travel through the nozzle instead of up the nozzle walls and through the reservoir-nozzle interface towards the threads. It is expected that different nozzle variations will continue to be fabricated and used with the injector to accommodate specific experiments and optimize droplet formation.

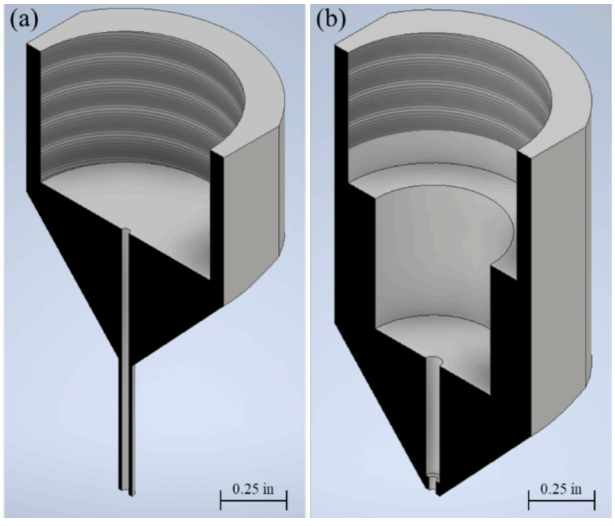

Fig. 4. Cross section views of the (a) original nozzle design used in the testing phase and the initial HIDRA-MAT experiments and (b) current design used in the droplet formation experiments.

The custom mounting flange connects the LBD and the liquid metal reservoir. The flange is a DN63CF (4.5″) to DN16CF (1.33″) zero-length reducer that has been modified for this application. Modifications include another DN16CF connection on the vacuum side of the flange that has tapped holes so the liquid metal reservoir can be securely attached. A hole was drilled through the flange and a half nipple with a DN16CF connection was welded onto the flange. On the atmospheric side of the flange, the LBD is connected to hold vacuum, but on the vacuum side, the connection does not contribute to maintaining vacuum, so the gasket can be reused. By reusing a gasket, the connection point provides an escape for any pressure that may build up in the reservoir when heating the metal and driving the piston. It was critical that the LBD and reservoir assembly were able to connect to a DN63CF to keep the design compact. When fully assembled, the LMDI is easily loaded with lithium and installed onto the LSM by a single person.

Droplets are produced by driving a piston with the LBD through the reservoir to push the molten lithium through the nozzle. The piston connects to the LBD and the LBD movement is controlled through a Nanotec Electronic C5–01 open-loop stepper motor controller. Piston actuation drives lithium out of the nozzle tip while the high surface tension of lithium prevents the droplet from falling. Surface tension allows multiple consecutive piston steps, enabling control of droplet size during formation. Each piston step increases the droplet to the desired size, and then the LSM is used to lower the droplet to the sample. Further data on droplet formation in HIDRA-MAT is presented in the "Droplet Formation Experiments in HIDRA-MAT" section. Fig. 5 shows all electrical connections for the injector.

2.3. Cleaning and refilling

With a loading mass of ~3.5 g, the LMDI can be cleaned and refilled in a day. Once testing has been completed, the piston is retracted to its home position, and HIDRA-MAT is brought up to atmospheric pressure. The LMDI is then removed from the LSM and the copper shim is removed from the nozzle. After removal of the LMDI, the reservoir assembly components (reservoir, nozzle, and piston) are detached from the mounting flange and the heating coil is removed from the reservoir. The LMDI components are then cleaned for ~30 min. At higher coil temperatures, small amounts of lithium can creep up the piston and bind the piston in place inside of the reservoir. In that case, the reservoir is removed by unscrewing the reservoir and piston as one piece and cleaned together. The components eventually separate during the cleaning process. In the case of droplet testing in HIDRA-MAT, the excess lithium was collected in HIDRA-MAT, removed, and then disposed of properly. Following cleaning, the components are dried, the glove box is prepared, and the LMDI is ready for lithium loading.

3. Experimental setup and results

3.1. Initial testing phase

The injector setup shown in Fig. 6 tested droplet formation and application with the first nozzle design. A test setup was initially used to protect equipment from potential liquid lithium spills in HIDRA-MAT during initial system calibration. This temporary setup provided all the necessary features to demonstrate that the injector would work when installed on HIDRA-MAT. Unannotated in Fig. 6 is the gate valve, turbomolecular pump, rough pump, and supporting electronics. After installing the injector onto the vacuum chamber, the supporting

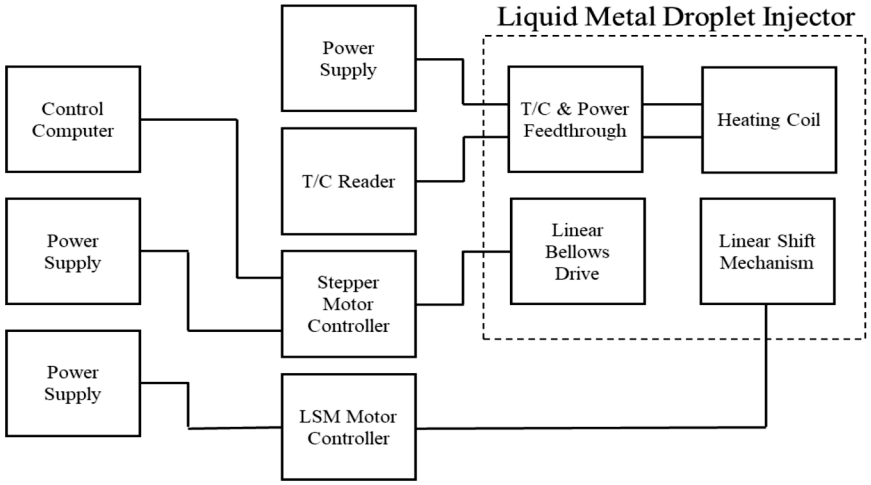

Fig. 5. Schematic of wiring connections for the LMDI. All operation of the LMDI can be carried out remotely if necessary.

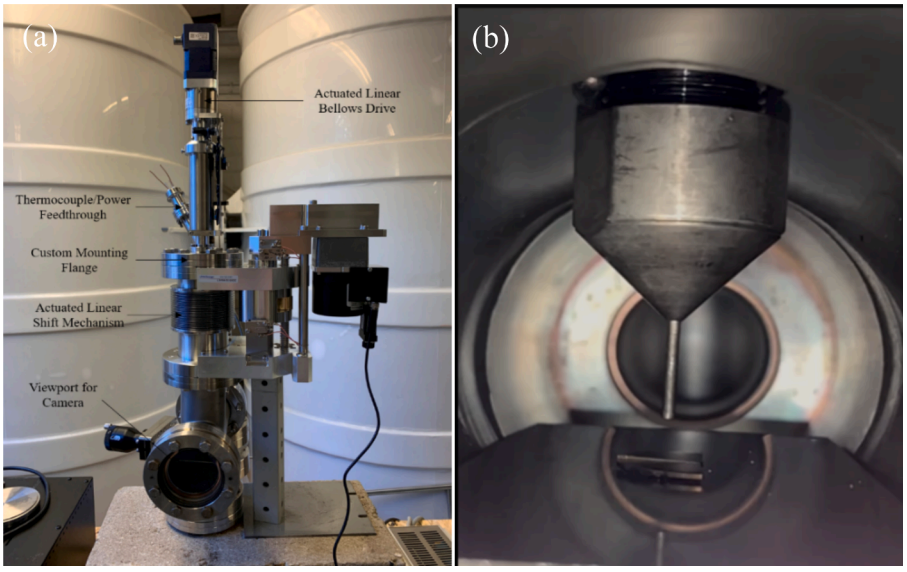

Fig. 6. Experimental setup of (a) the LMDI and (b) view looking at nozzle position above an unheated tungsten sample.

electronics for supplying power and reading/sending data were all connected. An external thermocouple monitored the temperature of the bellows during the heating of the coil for safety.

Before the LMDI was installed on the test vacuum chamber, it was loaded with lithium in an argon environment. Fig. 7 shows the LMDI in the glovebox after the lithium was loaded. The opening at the nozzle tip is covered during the transfer process to limit oxidation of the lithium. Purity was not a concern for these tests since minimal oxidation would

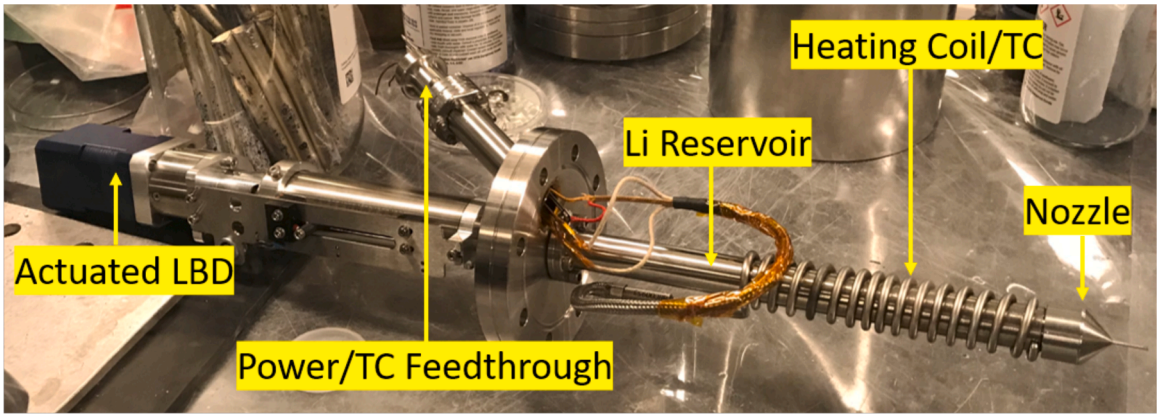

Fig. 7. The LMDI in the lithium loading glovebox, which provides an argon environment to mitigate oxidation of the lithium.

take place during installation and would not affect droplet formation. Furthermore, lithium use in commercial devices will have to deal with oxidation concerns, so there is validity to allowing minimal amounts of oxidation to mimic those conditions. If purity were to become a concern, the design would necessitate a vacuum suitcase for transfer.

Droplet diameters created during testing had a range of less than 1 mm for the three droplets shown in Fig. 8. The difference in droplet diameter can be explained by further describing the experimental procedure. When droplet one was formed, surface tension kept it attached to the nozzle. The droplet was then lowered to the surface of the unheated tungsten sample using the LSM. Once in contact with the substrate, the nozzle was retracted, leaving the droplet on the surface. If the sample were heated, it is expected that the droplet would more easily transfer to the sample through wetting. Understanding wetting behavior was not the purpose of this test or the other tests presented in this report.

Droplet two was formed with the nozzle retracted and aligned above the first droplet. Droplet two grew until it coalesced with the first droplet. This coalescence demonstrated that, even with impurity growth on the droplet surface, it had not cooled off or hardened sufficiently to prevent joining between droplets. The same effect was present for the application of the third droplet. Droplet three had a smaller diameter than droplet two. With the same actuation step program, it is expected that each droplet would be the same size. However, the combination of the first two droplets reduced the distance between nozzle and sample. This reduced distance caused droplet three to contact the coalesced droplet sooner, so the measured diameter of droplet three was smaller. If there were room for the full droplets to form, greater consistency in diameters would be anticipated.

Fig. 9 highlights the effects of lithium oxidation under high vacuum conditions. The application of the droplet to the substrate is shown in Fig. 9a. At the time of application, the droplet is hot and has a reflective surface signaling there are relatively low amounts of impurity present. As the droplet sits on the substrate, it starts to cool and undergoes oxidation. After one minute, lithium oxidation was observed by the change in the droplet's shell appearance, transitioning from reflective to dull, as seen in Fig. 9b. A lower pressure would slow this oxidation effect. The addition of a second droplet in Fig. 9c, four minutes after the first droplet, reveals that the first droplet had not become solid as droplet two was able to be absorbed into the first. There is a clear distinction in the shell of the two-droplet mass between the parts of the shell that originated from the first droplet and those of the added second droplet. Fig. 9d was captured directly after the addition of a third droplet. The third droplet was added one minute after the second. After adding the third droplet, the shell from the first droplet can still be distinguished, and the cooled and oxidized parts are in different positions of the lithium mass. It was observed that these cooled and oxidized shell parts rotated on the shell of the lithium mass when a new droplet was added. Furthermore, Fig. 9e was captured two minutes after the third droplet added, giving the coalesced droplet time to cool and oxidize in vacuum. It can be seen that the coalesced droplet had started to cool and oxidize, but even so, parts of the first droplet's shell can be observed in this last documented stage. Once the droplet was brought to atmosphere, the outer shell took on a uniform, matte appearance.

4. Droplet formation experiments in HIDRA-MAT

Experiments have been carried out in HIDRA-MAT using the second nozzle design to understand the formation of liquid lithium droplets on the nozzle at different nozzle temperatures and piston step sizes. Sample preparation allows for samples be heated to specific temperatures and may necessitate a specific amount of lithium to be applied to the sample. The three nozzle temperature setpoints that were chosen for these experiments were 185 °C, 230 °C, and 270 °C. The lower end of the temperature range is slightly above the melting temperature of lithium ($T_{melt,\ Li}$ = 180.5 °C) to ensure that cooling on the nozzle tip, which would cause clogging, was avoided. The higher end of the temperature range was chosen according to the most recent experimental campaign using HIDRA-MAT which required samples to be heated to ~270 °C. At each temperature, four piston step sizes were examined (0.125 mm, 0.25 mm, 0.5 mm, and 1 mm). Piston actuation control made reproducible step sizes straightforward to achieve. The range of step sizes were selected such that they were within a narrow enough range to be comparable and small enough that each would take multiple steps before a droplet detached from the nozzle. Droplet creation and detachment were captured on video and then analyzed with ImageJ software.

For each test, ~3 g of lithium was loaded into the reservoir and the LMDI was installed onto HIDRA-MAT. A thermocouple was placed into contact with the nozzle tip to measure the temperature. HIDRA-MAT was then pumped down overnight. The next morning, the heating coil was brought to its target temperature, the nozzle tip thermocouple was removed *in-vacuo*, and the LMDI was ready for use. This process was repeated for each test.

Final droplet size is an important metric in understanding droplet creation because it directly relates to nozzle-droplet interaction. Unlike some fast-droplet injectors that rely on gas back-pressure to create a stream of droplets [11], single-droplet injectors' droplet creation is considerably slower and nozzle-droplet interactions have more of an effect on droplet formation. The final droplet size in this test was determined by measuring the droplet that detached from the nozzle tip. For droplet detachment to occur in the LMDI, the droplet's weight has to overcome the surface tension force. As nozzle temperature increased, it

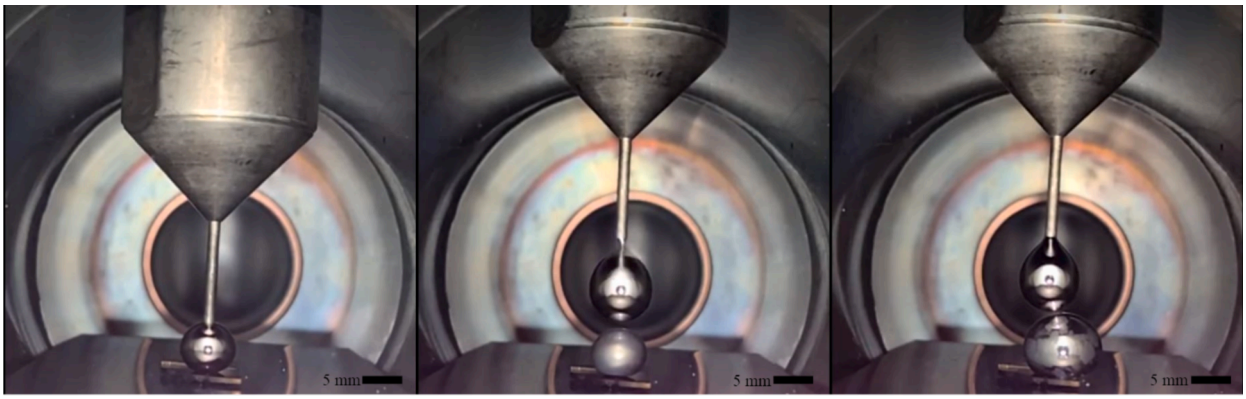

Fig. 8. Three droplets were produced during the experiment and their size was measured using ImageJ software. (For interpretation of the references to colour in this figure legend, the reader is referred to the web version of this article.).

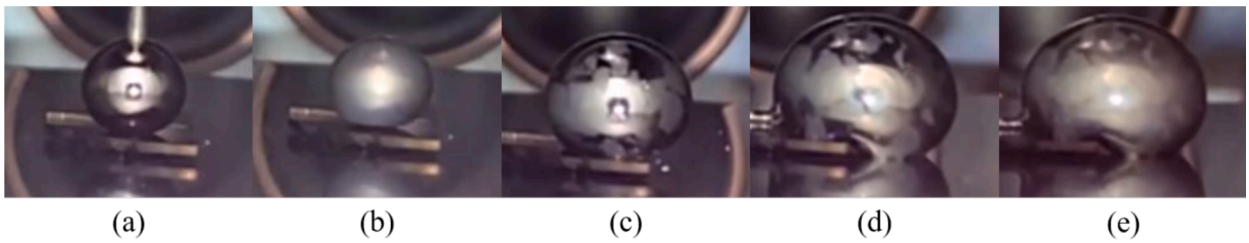

Fig. 9. Five points in time were chosen since the first droplet was applied: (a) Right at the time of application of the droplet to the sample, (b) letting time pass to observe oxidation, (c) addition of a droplet two, (d) addition of another droplet, and (e) letting time pass to observe oxidation.

was observed that the size of the final droplet increased. This can seem counterintuitive because the surface tension of lithium decreases with an increase in temperature [12]. However, it is known that the wetting properties of lithium onto stainless steel change with temperature [8]. As temperature increases, the lithium will better wet the stainless steel and creep up the nozzle walls as shown in Fig. 10. This creep will cause the surface area of the nozzle-lithium interface to increase and subsequently increase the force required for the droplet to detach. It can be inferred from Fig. 11 that with an increase in nozzle temperature, there is an increase in the force needed to overcome surface tension forces to cause droplet detachment. This increase results in droplets growing larger in size before detaching. If lithium creep was not present and the lithium-nozzle interface surface area was constant, it would be expected that the relationship would be the inverse and final droplet diameter would decrease with an increase in nozzle temperature.

In addition to understanding droplet size with increases in temperature, four different step sizes were investigated (0.125 mm, 0.25 mm, 0.5 mm, and 1 mm). Fig. 12 presents final droplet sizes created from the same step size across increasing nozzle temperatures. As explained previously, droplet diameter increases with nozzle temperature, and it is observed that step size has no effect on that trend. Comparing each step size at specific temperatures revealed no discernable trends in final droplet size. However, Fig. 13 does confirm that smaller step sizes require more steps for the droplet to detach, as expected. For a step size of 0.125 mm, the number of steps required until detachment approximately doubled with each increase in temperature. The data presented in Fig. 13 shows the first look at droplet formation correlations with the second nozzle design at each temperature and step size. This data can be utilized as a reference for future experiments that may require a known amount of lithium on the sample.

Droplet size control may be required for some experiments and, as can be seen from Fig. 14, the LMDI has the ability to control droplet size on the substrate. Each droplet was formed on the nozzle and then

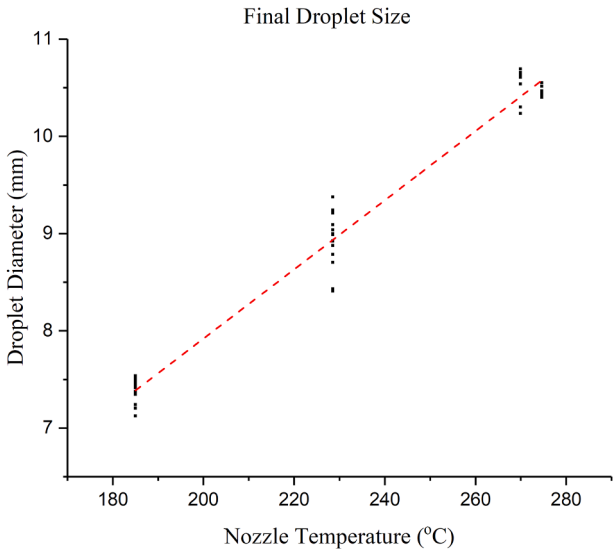

Fig. 11. Across all temperatures and step sizes, the diameter of the droplet that detached from the nozzle was recorded. As nozzle tip temperature increased, so did the final droplet size. For data between temperature setpoints to be compared, two separate tests were carried out at the 270 °C setpoint.

applied to the substrate using the LSM. The substrate was then moved with the HIDRA-MAT transfer arm and the process was repeated. Sixteen droplets in total, four sets of four, were applied to the Kapton substrate. When using the LMDI in an experiment, the maximum number of droplets available depends on the experimental objective and setup which considers factors such as droplet size and substrate length. Each droplet in sets one, two, three, and four were created by one, two, three,

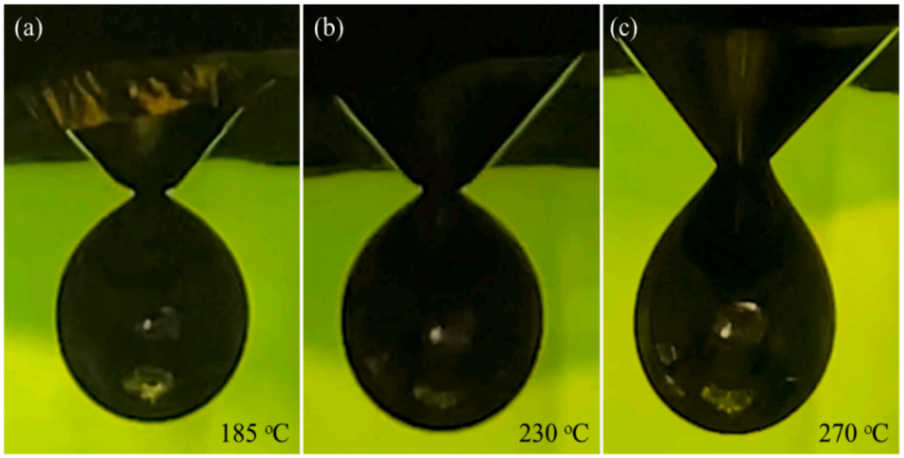

Fig. 10. The images above show an increase in nozzle wetting with an increase in nozzle temperature. At (a) 185 °C the nozzle-droplet interface is clearly defined. As nozzle temperature increases to (b) 230 °C and (c) 270 °C the lithium droplet begins to wet the nozzle tip and starts to creep up the outside of the nozzle.

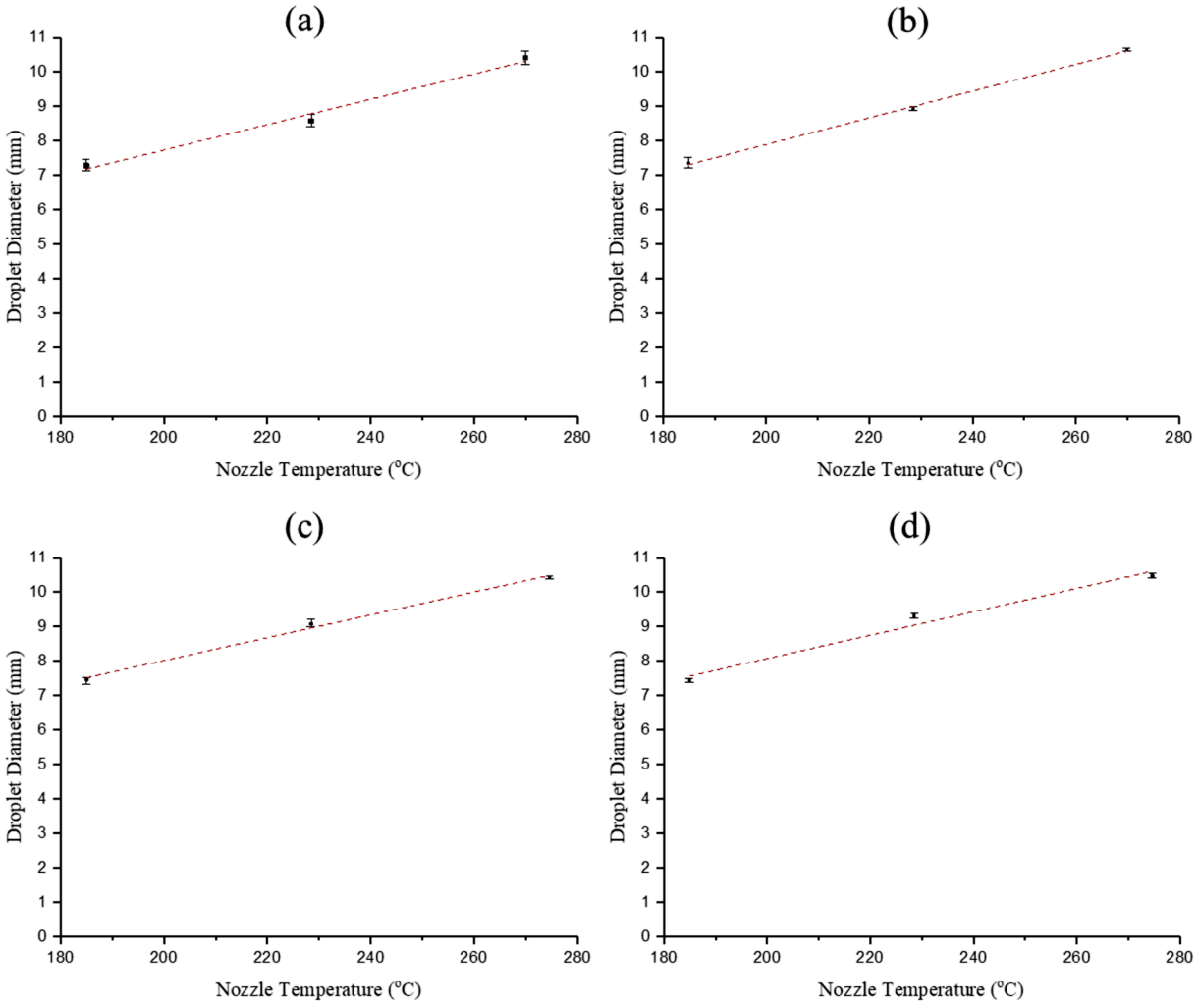

Fig. 12. Each graph represents final droplet diameter based on step sizes (a) 0.125 mm, (b) 0.25 mm, (c) 0.5 mm, and (d) 1 mm over temperature. Each data point represents an average value of all collected points at that temperature for that step size. Range bars represent the maximum and minimum diameters for each data set.

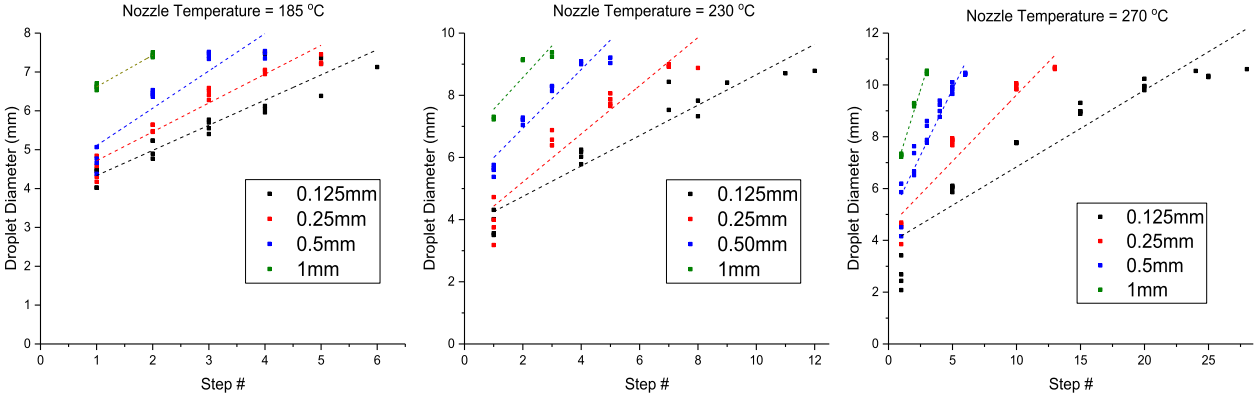

Fig. 13. Each graph shows the number of piston steps required to detach the droplet from the nozzle. Every droplet was measured and plotted at each temperature and step size. (For interpretation of the references to colour in this figure legend, the reader is referred to the web version of this article.).

and four piston steps, respectively. The average diameter of droplet sets one, two, three, and four were 3.04 ± 0.14 mm, 3.99 ± 0.10 mm, 4.72 ± 0.13 mm, and 5.10 ± 0.06 mm respectively. The measured diameters were then used to calculate the mass of each droplet. The average mass of droplet sets one, two, three, and four were 7.88 ± 1.1 mg, 17.84 ± 1.36 mg, 29.44 ± 2.37 mg, and 37.02 ± 1.41 mg, respectively. Though there was a small amount of variance in droplet shape which occurred from the application of the droplets onto the cold Kapton substrate, size control was demonstrated. The majority of experiments in HIDRA-MAT will only require one droplet to be formed and applied to a substrate. Nevertheless, the LMDI has demonstrated precise control over droplet formation as demonstrated through the presented measurements and

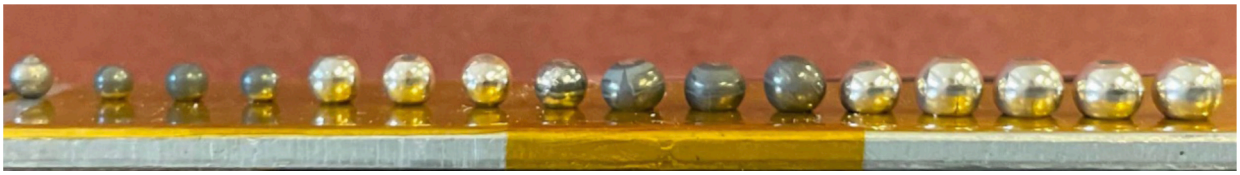

Fig. 14. An example of lithium droplet control onto a substrate. In this case, the substrate was unheated Kapton. From left to right, the number of steps before application to the substrate was increased every four droplets. The first four droplets were applied after one step at 180 °C and the last four droplets were applied after four steps at 180 °C. Differences in color are from oxidation effects after the lithium was taken out of vacuum.

the ability to create multiple consecutive droplets. However, the data set is small, and more testing is required to establish certainty at different temperature setpoints for each nozzle design.

5. Conclusion

An LMDI was designed and fabricated for use on HIDRA-MAT to aid in the study of liquid metal PFC materials. A compact and straightforward design makes the injector robust and compatible with different substrate types and sizes. The LMDI has a loading capacity of ~3.5 g of lithium, which has proven to be a sufficient amount for HIDRA-MAT experiments. Automatic actuation of the reservoir piston and LSM motion have demonstrated safe operation and control of droplet size over a range of different nozzle temperatures (180 °C – 270 °C). Initial experiments on a temporary vacuum chamber determined the injector could reproduce droplets of diameters within ~0.8 mm of each other. Cooling and impurity effects were present during testing and provided insight into how the liquid lithium interacts with an unheated substrate and other droplets. Following proof of concept, the LMDI was utilized in HIDRA-MAT to investigate the formation of droplets with a second nozzle design. It was found that as nozzle temperature increased, the size of the liquid metal droplet that detached from the nozzle became larger. This behavior is attributed to a combination of nozzle design and increased wetting of lithium on stainless-steel at higher temperatures. Future nozzle designs can be implemented to explore if droplet formation behavior can correlate with surface tension such that the detached droplet size decreases with an increase in temperature due to the decrease in surface tension. Droplet formation effects due to step size were studied as well. It was shown that smaller step sizes required more steps to observe droplet detachment from the nozzle when compared with larger step sizes. Lastly, the LMDI demonstrated the ability to control droplet diameter and apply multiple droplets to an unheated substrate with ± 0.14 mm accuracy between droplets of the same set. Supported by the results presented here, the HIDRA-MAT LMDI provides a unique opportunity for the expansion of current liquid metal PFC research. The LMDI is an advancement of current single-droplet injectors and will aid in developing liquid metal PFCs, as well as being utilized for other studies involving liquid metal-substrate interactions of interest.

CRediT authorship contribution statement

A. Shone: Conceptualization, Methodology, Investigation, Resources, Formal analysis, Writing – original draft, Writing – review & editing, Visualization. **Z. Koyn:** Resources, Writing – original draft, Writing – review & editing, Supervision, Funding acquisition. **B. Kamiyama:** Investigation, Formal analysis, Writing – review & editing. **E. Perez:** Formal analysis. **L. Barrus:** Formal analysis. **N. Bartlett:** Investigation. **J.P. Allain:** Writing – original draft, Supervision, Funding acquisition. **D. Andruczyk:** Writing – original draft, Supervision, Funding acquisition.

Declaration of Competing Interest

The authors declare that they have no known competing financial interests or personal relationships that could have appeared to influence the work reported in this paper.

Acknowledgments

This work is supported by the Department of Energy [DESC0017719].

References

[1] P. Fiflis, N. Connolly, D. Ruzic, Experimental mechanistic investigation of the nanostructuring of tungsten with low energy helium plasmas, J. Nucl. Mater. 482 (2016) 201–209.
[2] D. Andruczyk, R. Maingi, J.S. Hu, et al., Overview of lithium injection and flowing liquid lithium results from the US–China collaboration on EAST, Phys. Scr. T171 (2020).
[3] R. Maingi, R. Majeski, J.E. M.enard, et al., Lithium as a plasma facing component to optimize the edge plasma, in: 2015 IEEE 26th Symposium on Fusion Engineering (SOFE), Austin, TX, 2015, pp. 1–5.
[4] D.N. Ruzic, W. Xu, D. Andruczyk, et al., Lithium–metal infused trenches (LiMIT) for heat removal in fusion devices, Nucl. Fusion 51 (2011), 102002.
[5] A.L. R.oquemore, D. Andruczyk, R. Majeski, et al., Upward-facing lithium flash evaporator for NSTX-U, in: 2013 IEEE 25th Symposium on Fusion Engineering (SOFE), San Francisco, CA, 2013, pp. 1–5.
[6] A. Nagy A. Bortolon, E.P. G.ilson, et al., Lithium granular injector operational experience triggering ELMs in H-mode on DIII-D, in: 2015 IEEE 26th Symposium on Fusion Engineering (SOFE), Austin, TX, 2015, pp. 1–6.
[7] D.K. Mansfield, A.L. Roquemore, H. Schneider, et al., A simple apparatus for the injection of lithium aerosol into the scrape-off layer of fusion research devices, Fusion Eng. Des. 85 (2010) 890–895.
[8] P. Fiflis, A. Press, W. Xu, et al., Wetting properties of liquid lithium on select fusion relevant surfaces, Fusion Eng. Des. 89 (2014) 2827–2832.
[9] M.J. Baldwin, T. Lynch, L. Chousal, et al., An injector device for producing clean-surface liquid metal samples of Li, Ga and Sn–Li in vacuum, Fusion Eng. and Des. 70 (2) (2004) 107–113.
[10] A. Shone, Z. Koyn, R. Rizkallah, et al., An Overview of the Hybrid Illinois Device for Research and Applications Material Analysis Test-stand (HIDRA-MAT), J. Fusion Energy 39 (2020) 448–454.
[11] D. Andruczyk, A.L. Roquemore, P. Fiflis, et al., A Method to Produce Lithium Pellets for Fueling and ELM Pacing in NSTX-U, Fusion Eng. Des. 89 (2014) 2910–2914.
[12] H. Davison, Compilation of Thermophysical Properties of Liquid Lithium, NASA Technical Report NASA TN D-4650 (1968).